26th EPS Conf. on Contr. Fusion and Plasma Physics, Maastricht, 14 - 18 June 1999 ECA Vol.23J (1999) 1245 - 1248

Modeling of Trapped Electron Effects on Electron Cyclotron Current Drive for Recent DIII-D Experiments

Y.R. Lin-Liu,[1] O. Sauter,[2] R.W. Harvey,[3] V.S. Chan,[1] T.C. Luce,[1] R. Prater[1]

[1]*General Atomics, P.O. Box 85608, San Diego, California 92186-5608, U.S.A.*
[2]*CRPP, Ecole Polytechnique Fédérale de Lausanne, 1007 Lausanne, Switzerland*
[3]*CompX. 12839 Via Grimaldi, Del Mar, California 92014*

Owing to its potential capability of generating localized non-inductive current, especially off-axis, Electron Cyclotron Current Drive (ECCD) is considered a leading candidate for current profile control in achieving Advanced Tokamak (AT) operation. In recent DIII–D proof-of-principle experiments [1], localized off-axis ECCD has been clearly demonstrated for first time. The measured current drive efficiency near the magnetic axis agrees well with predictions of the bounce-averaged Fokker-Planck theory [2,3]. However, the off-axis current drive efficiency was observed to exceed the theoretical results, which predict significant degradation of the current drive efficiency due to trapped electron effects. The theoretical calculations have been based on an assumption that the effective collision frequency is much smaller than the bounce frequency such that the trapped electrons are allowed to complete the banana orbit at all energies. The assumption might be justified in reactor-grade tokamak plasmas, in which the electron temperature is sufficiently high or the velocity of resonant electrons is much larger than the thermal velocity, so that the influence of collisionality on current drive efficiency can be neglected. For off-axis deposition in the present-day experiments, the effect of high density and low temperature is to reduce the current drive efficiency, but the increasing collisionality reduces the trapping of current-carrying electrons, leading to compensating increases in the current drive efficiency. In this work, we use the adjoint function formulation [4] to examine collisionality effects on the current drive efficiency.

By using the adjoint techniques to discuss current drive efficiency, we are assuming that the plasma is close enough to the Maxwellian equilibrium, *i.e.*, $f \sim f_{\mathrm{M}}$, for the collision operator to be linearized, and that the rf power density is not too high such that interactions between the EC waves and electrons can be described by $S_{\mathrm{rf}}(f_{\mathrm{M}})$, where S_{rf} denotes the rf quasilinear diffusion operator. The perturbed distribution function f_1 satisfies the linearized Fokker-Planck equation:

$$\mathrm{v}_{\|}\hat{b}\cdot\nabla f_1 - C_{\mathrm{e}}^{\ell} f_1 = S_{\mathrm{rf}}(f_{\mathrm{M}}) \ , \tag{1}$$

The parallel driven current density $j_{\|} = -e\int d\Gamma\, f_1 \mathrm{v}_{\|}$. It can be shown that $j_{\|}/B$ is a flux-surface quantity. Rather than solving Eq. (1) directly, we consider the adjoint problem:

$$-\mathrm{v}_{\|}\hat{b}\cdot\nabla\chi - C_{\mathrm{e}}^{\ell +}\chi = \frac{\mathrm{v}_{\|}B}{\langle B^2\rangle} \ , \tag{2}$$

where $C_{\mathrm{e}}^{\ell +}$ is the adjoint collision operator and $\langle \ldots \rangle$ denotes the flux surface average. For a given flux surface χ is a function of energy ($w = \gamma mc^2 = mc^2[1+(u/c)^2]^{1/2}$), $\vec{u} \equiv \vec{p}/m$, magnetic moment ($\mu = m\mathrm{u}_\perp^2 / 2B$), $\sigma = \mathrm{sgn}(u_\parallel)$, and poloidal angle θ_p. The rf-driven current density is then given $j_\parallel = -eB\langle \int d\Gamma\, \chi S_\mathrm{rf}(f_\mathrm{M})\rangle$. We express the current drive efficiency η as

$$\frac{\eta}{T_\mathrm{e}} \equiv \frac{n_\mathrm{e}\langle j_\parallel \rangle}{2\pi Q} = \frac{4\varepsilon_0^2}{e^3 \ell n\Lambda}\left\langle \frac{B}{B_\mathrm{max}} \right\rangle \frac{\langle \int d\Gamma\, \tilde{\chi} S_\mathrm{rf}(f_\mathrm{M})\rangle}{\langle \int d\Gamma (w / m\mathrm{v}_\mathrm{e}^2) S_\mathrm{rf}(f_\mathrm{M})\rangle} \ , \tag{3}$$

where Q is absorbed rf power density, and $\tilde{\chi} = \nu_\mathrm{e0}(B_\mathrm{max} / \mathrm{v}_\mathrm{e})\chi$ with $\mathrm{v}_\mathrm{e} = (2T_\mathrm{e} / m)^{1/2}$ and $\nu_\mathrm{e0} = (e^4 n_\mathrm{e} \ell \mathrm{n}\Lambda) / (4\pi\varepsilon_0^2 m^2 \mathrm{v}_\mathrm{e}^3)$. Note that the formulation is applicable for an arbitrary collisionality and in general tokamak geometry. The adjoint function χ, once evaluated, can also be used to calculate the neoclassical conductivity and bootstrap current [5]. To solve Eq.(2) with the full Coulomb collision operator is a three-dimension numerical problem.

In the large aspect ratio limit, $\delta \equiv r/R \to 0$, analytic solutions is possible. Write $\chi = \chi_\mathrm{c} + \chi_\mathrm{t}$, where χ_c satisfies the equation $-C_\mathrm{e}^{\ell+}\chi_\mathrm{c} = \mathrm{v}_\parallel B / \langle B^2 \rangle$ and χ_t can be identified as the trapped-electron contribution. Note that χ_c is proportional to the Spitzer function is the straight field-line geometry and χ_t can be determined by considering the pitch-angle scattering only for $\delta << 1$. Then, it is straightforward to calculate the banana regime solution of χ_t. The leading order correction to the banana regime result can be obtained using the boundary-layer analysis of Hinton and Rosenbluth [6]. The boundary-layer contribution to the ECCD efficiency is found to be [7]

$$\Delta j_\parallel \cong (\nu_* \delta)^{1/2} j_\mathrm{c} \ , \tag{4}$$

where j_c is the driven current calculated using χ_c, and $\nu_* = \sqrt{2}(qR) / (\delta^{3/2}\tau_\mathrm{e}\mathrm{v}_\mathrm{e})$ with τ_e the Braginskii collision time and q the safety factor.

To account for effects of finite aspect ratio, we calculate χ using Fisch's relativisitic high-velocity collision model [8]:

$$C_\mathrm{e} f \approx \left[\nu_\mathrm{ei}(u) + \nu_\mathrm{D}(u)\right] Lf + \frac{1}{u^2}\frac{\partial}{\partial u} u^2 \lambda_\mathrm{s}(u) f \ , \tag{5}$$

where L is pitch-angle scattering operator, $\nu_\mathrm{ei}(u) = Z_\mathrm{eff}\, \nu_\mathrm{e0}\gamma(u_\mathrm{e} / u)^3$, $\nu_\mathrm{D}(u) = \nu_\mathrm{e0}\gamma(u_\mathrm{e} / u)^3$, and $\lambda_\mathrm{s}(u) = \nu_\mathrm{e0} u_\mathrm{e}\gamma^2 (u_\mathrm{e} / u)^2$ with $u_\mathrm{e} \equiv \mathrm{v}_\mathrm{e}$. In the banana regime, *i.e.*, $\nu_* \to 0$,

$$\chi \to \chi_\mathrm{b} = \mathrm{sgn}(u_\parallel) H(\lambda) G(u, Z_\mathrm{eff}, f_\mathrm{t}) \ , \tag{6}$$

$$H(\lambda) = \frac{\theta(\lambda_c - \lambda)}{2} \int_\lambda^{\lambda_c} \frac{d\lambda'}{\langle (1 - \lambda' B)^{1/2} \rangle} \ , \tag{7}$$

$$G(u, Z_\mathrm{eff}, f_\mathrm{t}) = \left(\frac{c^2}{\nu_\mathrm{e0} u_\mathrm{e}^3}\right) \frac{1}{(1 - f_\mathrm{t})} \left(\frac{\gamma + 1}{\gamma - 1}\right)^{\hat{\rho}/2} \int_0^\gamma d\gamma' \left(\frac{u'}{\gamma'}\right)^2 \left(\frac{\gamma' - 1}{\gamma' + 1}\right)^{\hat{\rho}/2} \ , \tag{8}$$

with $\lambda = B^{-1}(u_\perp / u)^2 = B^{-1}(1 - \xi^2)$, $\lambda_c = B_\mathrm{max}^{-1}$, $\hat{\rho} = (Z_\mathrm{eff} + 1) / (1 - f_\mathrm{t})$, and $f_\mathrm{t} = 1 - 3/4 \langle B^2 \rangle \int_0^{\lambda_c} \langle (1 - \lambda' B)^{1/2} \rangle^{-1} \lambda' d\lambda'$, the effective trapped-particle fraction. We have found that χ given in Eq. (5) gives similar predictions of ECCD as those of Ref. 2. In the limit of $\nu_* >> 1$, $\chi \to \chi_c = (B/\langle B^2 \rangle)\xi G(u, Z_{eff}, f_t = 0)$. For a finite ν_*, we propose to approximate χ by the interpolation formula:

$$\chi \approx \chi_c + \left(1 + \alpha\sqrt{\nu_*}\left(\frac{u_e}{u}\right)^2\right)^{-1} (\chi_b - \chi_c) \ , \tag{9}$$

where α is an adjustable parameter. We determine α by making use of Eq. (9) to calculate the neoclassical conductivity σ_{neo} and the density-gradient bootstrap current coefficient L_{31} for the Lorentz-gas model ($Z_{eff} >> 1$). That $\alpha = 2$ gives $\sigma_{neo} / \sigma_{sp} = 1 - f_t / [1 + 0.59(\nu_*)^{1/2}]$ and $L_{31} = f_t / [1 + (\nu_*)^{1/2}]$, which agree well with the recent numerical results of Ref. 5 for these two transport coefficients.

Using the kinetic profiles and the ECH system parameters of recent DIII–D experiments [1], we have calculated the collisionality correction to the ECCD efficiency by applying Eqs. (3) and (9). We have also calculated the corresponding ECCD efficiencies in both the collisional ($\nu_* >> 1$) and collisonless ($\nu_* = 0$) limits. Typical experimental density and temperature profiles are shown in Fig. 1(a). The corresponding collisionality parameter is shown in Fig. 1(b). Comparison of the theoretical and experimental ECCD results are shown in Fig. 2 , Fig. 2(a) for the near magnetic axis cases and Fig. 2(b) for the off-axis ECCD. The collisionality correction appears to be consistent with predictions of Eq. (4) and gives modest improvement in the current drive efficiency in comparison with the collisionless value. The collisionality correction gives modest improvement in the current drive efficiency in comparison with the collisionless value. Good agreement between the theoretical and experimental results is observed in the near magnetic axis cases. But in the off-axis cases, experimental data appear to be more consistent with the theoretical results of $\nu_* >> 1$.

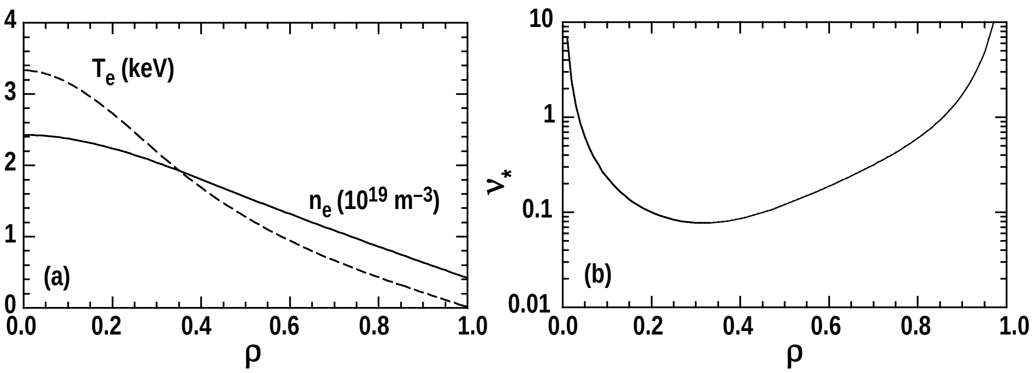

Fig. 1. (a) Experimental density and temperature profiles of an off-axis ECCD discharge; (b) the corresponding ν_* as a function of normalized minor radius ρ.

In summary, we have estimated the collisonality effect on ECCD efficiency using a velocity-space connection formula. The collisionality correction provides a modest improvement in the efficiency, but only partially resolves the discrepancy between the observed experimental values and the previous theoretical results for off-axis current drive.

This work was supported by the U.S. Department of Energy under Contract DE-AC03-99ER54463 and in part by the Swiss National Science Foundation.

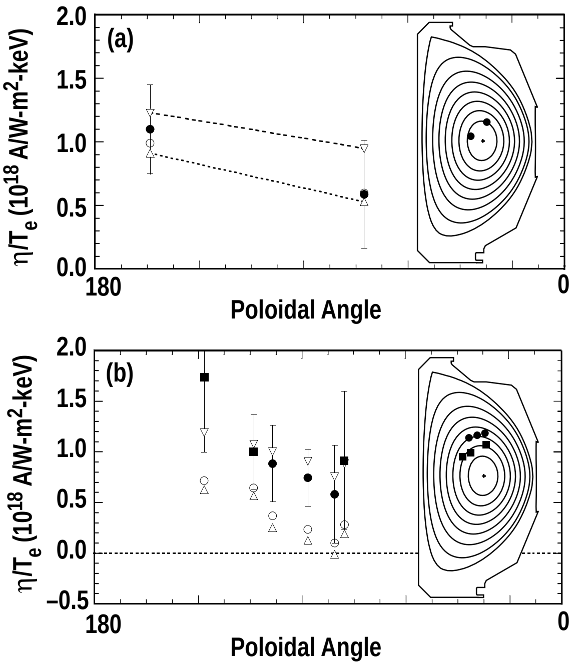

Fig. 2. Comparison of theoretical and experimental values of normalized off-axis ECCD efficiency n / T_e as function of poloidal angle. $\nu_* >> 1$ is shown by inverted triangles and $\nu_* = 0$ by regular triangles; open circles represent interpolation at ν_* (exp.). (a) Near magnetic axis cases (solid circles indicate $\rho = 0.16$, 0.24); (b) off-axis cases (solid circles indicate $\rho = 0.47$ and solid squares indicate $\rho = 0.34$).

References

[1] Luce, T.C., *et al.*, ‘‘Current Profile Modification with Electron Cyclotron Current Drive in the DIII–D Tokamak,’’ to be published in *Proc. IAEA Meeting*, Yokohama, 1998 (International Atomic Energy Agency, Vienna, 1999).

[2] Cohen, R.H., *Phys. Fluids* **30,** 2442 (1987).

[3] Harvey, R.W., McCoy, M.C., ‘‘The CQL3D Fokker-Planck Code,’’ in *Advances in Simulation and Modeling of Thermonuclear Plasmas* (Proc. IAEA Technical Committee Meeting, Montreal, 1992), IAEA, Vienna (1993), p. 498.

[4] Antonsen, T.M., Jr., Chu, K.R., *Phys. Fluids* **25**, 1295 (1982).

[5] Sauter, O., *et al.*, ‘‘Neoclassical Conductivity and Bootstrap Current Formulae for General Axisymmetric Equilibria and Arbitrary Collisionality Regime,’’ CRPP Report LRP 630/99 (1999).

[6] Hinton, F.L., Rosenbluth, M.N., Phys. Fluids **16**, 836 (1973).

[7] Chan, V.S., S.C. Chiu, S.C., APS (1981).

[8] Fisch, N.J., Phys. Ref. A **24**, 3245 (1981).